

Design and Analysis of Reed Solomon Code in 5G Release 18 Mobile Wireless Communication Technology

Muhamad Asvial  and Primayoga Budyprawira *

Department of Electrical Engineering, Faculty of Engineering, University of Indonesia, Depok, Indonesia
Email: asvial@eng.ui.ac.id (M.A.); pbudyprawira@gmail.com (P.B.)

*Corresponding author

Abstract—5G Technology is prone to channel noise during transmission due to its wireless communication nature. The channel's noise can alter the transmitted signal resulting in data errors on the receiving end. Burst error is a type of data error that produces errors in a localized manner, meaning the errors are close to each other for a certain length of time. The Forward Error Correction (FEC) methods used in 5G Communication are Low Density Parity Check (LDPC) and Polar Code which have great encoding and decoding performance, however, these FEC methods have lesser performance on channels that induce burst error. This research proposed a Reed-Solomon (RS) Code and Polar-RS Concatenation Code implementation on 5G Technology. RS Code and Polar Code concatenation will create an FEC that inherits the burst error correction capability of RS Code and the low complexity of Polar Code. The BER and throughput performance of RS and Polar-RS will be compared to LDPC in the Additive White Gaussian Noise (AWGN) channel and burst error channel (Gilbert-Elliot Channel). The Bit Error Rate (BER) results in Gilbert-Elliot Channel of Polar-RS Code is 10^{-8} when E_b/N_0 equals 0 dB and E_b/N_0 , equals 8 dB for RS Code. Compared to LDPC with a BER value of 10^{-8} when E_b/N_0 is 13 dB, Polar-RS and RS Code have superior BER performance on the burst error channel. The simulation of 5G Physical Downlink Shared Channel (PDSCH) on the Gilbert-Elliot channel using Polar-RS results in a throughput value of 100 % when E_b/N_0 equals 6dB whereas 5G PDSCH that uses LDPC has a throughput value of 100 % when E_b/N_0 equals 11 dB. The proposed Polar-RS Code can solve the LDPC's poor BER and throughput performance on burst error cases so that Polar-RS Code can be a good candidate for the future release of the 5G Communication System's FEC.

Keywords—reed-solomon code, polar-RS code, 5G, burst error, forward error correction

I. INTRODUCTION

5G Communication is a mobile wireless technology defined by 3GPP LTE Release 15 standard [1, 2]. This technology has three pillars of service delivery which are, eMBB that explains that 5G technology uses broadband communication that delivers fast data rate transfer, URLLC which explains that 5G technology has high

reliability and low latency, and Massive Machine-Type Communication (mMTC) which explains that 5G technology can provide large coverage of connectivity and the ability to connects large amounts of users both human and non-human [3, 4].

5G system has many channels to transmit different kinds of data. Physical Downlink Shared Channel (PDSCH) is one of the channels used to transmit downlink data from gNodeB to the user equipment [5].

PDSCH uses Quadrature Phase Shift Keying (QPSK), 16 Quadrature Amplitude Modulation (QAM), 64 QAM, and 256 QAM to modulate the carrier signal [6]. This channel also uses Low Density Parity Check (LDPC) for its Forward Error Correction (FEC) method.

Data transmission through wireless communication is prone to channel noise that can produce errors on the receiving end. One type of error that often happens is burst error where the error is close together in respect of time. One of the causes of burst error is the multiplexing process especially Orthogonal Frequency Division Multiplexing (OFDM) [7–9]. OFDM is used in the 5G communication system, hence, to ensure the performance of a 5G system, FEC methods are used in the 5G system.

5G Communication uses LDPC and Polar Code as its FEC. LDPC is used for data signal transmission and Polar Code is used for control signal transmission [10–14]. These two FECs are used in this communication technology because of their fast encoding and decoding process [15] and good error correction capability. However, these FEC methods have lesser performance in burst error channels [16].

Burst error can be modeled using a Gilbert-Elliot channel model [16, 17]. This channel model uses a two-state Markov model to represent two channel states, the bad state, and the good state as illustrated by Fig. 1 [16]. The bad state represents a channel with a high probability of error and the good state represents a channel with a low probability of error. The channel's state change is governed by a set of state probabilities. These state changes can produce a burst error pattern in some transmitted data. The good state represents the Additive

White Gaussian Noise (AWGN) channel with a high E_b/N_0 value whereas the bad state represents the AWGN channel with a low E_b/N_0 value.

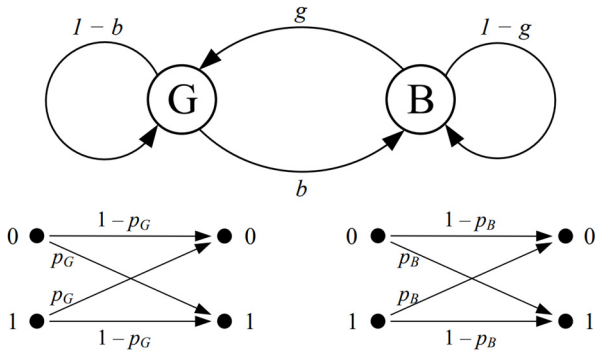


Fig. 1. Binary two-states Gilbert-Channel Elliot model [16].

The Reed Solomon Code is a family of block codes that create parity check bits for each symbol [18–22]. The parity check bits are generated by using arithmetic in Galois Field [23–28]. This algorithm makes Reed-Solomon Code have a superior performance in a burst error condition. The usage of Galois Field in the decoding and encoding process makes Reed-Solomon Code has slower decoding and encoding process compared to LDPC [16].

The LDPC has lesser performance in some cases of the Gilbert-Elliot Model Channel compared to Reed-Solomon Code based on the comparison of LDPC with message word lengths of 127 and 173 and the Reed-Solomon Code with the architecture of RS (127, 63) and (255, 127) [16]. The Reed-Solomon (RS) Code can be implemented as the replacement of the LDPC code, The only problem is the RS encoding and decoding process time that must be shortened to be able to have the same or faster than the encoding and decoding process of LDPC [29].

To lower the decoding and encoding complexity and improve the decoding performance, RS Code and Polar Code are concatenated [30]. Hence error correction capability from each FEC can be achieved with lower complexity.

The Bit Error Rate (BER) performance of LDPC and Reed-Solomon Code has been simulated through the Additive White Gaussian Noise (AWGN) channel in various papers [31–33]. This paper will simulate BER performance LDPC, RS code, and Polar-RS code communication through AWGN and Gilbert-Elliot Channel. Each FEC method’s performance in both channels will be directly analyzed and compared so that the best FEC method can be determined. Furthermore, the determined FEC will be simulated as the FEC block in a 5G PDSCH system and the throughput will be measured. This ensures the determined FEC performance in the 5G system is better than the current 5G FEC. The usage of better-performance FEC will result in better throughput and delay in data transmission over the 5G network.

This experiment focused on the LDPC’S low performance on burst error channel (Gilbert-Elliot). The proposed solution for that problem is using Reed-Solomon Code and Polar-RS code for replacing LDPC. The

measured performance is BER and throughput. The BER and throughput values will indicate the FEC’s performance in both AWGN Channel and Gilbert-Elliot Channel. Section II discusses related work concerning on Reed-Solomon Code, Polar-RS code, and LDPC BER Performance on AWGN and Gilbert-Elliot Channel, Section III discusses the proposed model and measurement model of this experiment, Section IV discusses the simulation result, and Section V discusses the conclusion of this experiment.

II. LITERATURE REVIEW

This paper focused on the LDPC’S poor performance on burst error channels. Other FEC alternatives are considered to find a better FEC’S performance than LDPC, so that, the FEC can replace LDPC on 5G Communication Technology. This will make 5G Communication more robust and have higher throughput.

A. Various Coding Scheme Comparison

LDPC is an FEC that consists of parity check matrices. LDPC has great error correction performance while using an iterative decoding algorithm [29]. LDPC has high effectiveness due to its low decoding complexity.

LDPC has a great error-correcting performance in the Gilbert-Elliot channel [29]. The Reed-Solomon Code produces the least error decoding probability for considering Gilbert channel parameters, however, in Gilbert-Elliot Channel with errors in a “good” state, LDPC performance is more effective [16]. This can be interpreted as the Reed-Solomon Code having superior performance when dealing with burst error “bad” state, but LDPC has better performance when dealing with “good” state error [16].

B. Polar Code Interleaving and Decoding Schemes Comparison

Polar Code is an FEC that maps the message word into different kinds of virtual polarized channels [8]. Every codeword K bit has its own K most reliable channels [8]. The reliable channel is used to transmit the message, and the rest is for the frozen bit. The Polar Code has low complexity compared to the Reed-Solomon code. Polar Code also solves the error floor problem that happened in LDPC. The computation time for polar code is more stable than LDPC codes in varying environments and for different code length [34].

A model of FEC which consists of a polar code with an outer BCH code is proposed [35]. The said model is tested for its BER performance for Random Interleaving (RI) and Blind Interleaving (BI) [35]. The research concludes that the BI scheme has better performance than the RI scheme, moreover, the BCH-Polar concatenated code performs better than the concatenated LDPC but performs worse than the concatenated Turbo code [35, 36].

C. Polar-RS Concatenation Code

A model FEC which consists of a concatenation of the Reed-Solomon Code and Polar code with threshold is proposed [37]. The proposed model has a high decoding

performance, low decoding complexity, and short latency [37]. In their paper, the improved concatenation scheme gives a coding gain advantage of 0.4 dB, and it can reduce the average number of RS codewords by 65 % and decrease the decoding latency by 50 % when the Signal to Noise Ratio (SNR) is 1.75 dB.

Compared to LDPC, Polar code has more stable decode and encode time. The computation times of Polar codes are about 3 times compared to LDPC codes at E_b/N_0 of 5 dB [34]. The better performance of RS code in Burst error case and the better performance of Polar Code computation make the Polar-RS code is proposed to be used in 5G transmission.

The proposed Polar-RS Concatenation uses the Reed-Solomon Code as the outer layer of the FEC and the Polar Code as the inner code. The codeword produced by the Reed-Solomon code is interleaved before it is coded with polar code as shown in Fig. 2.

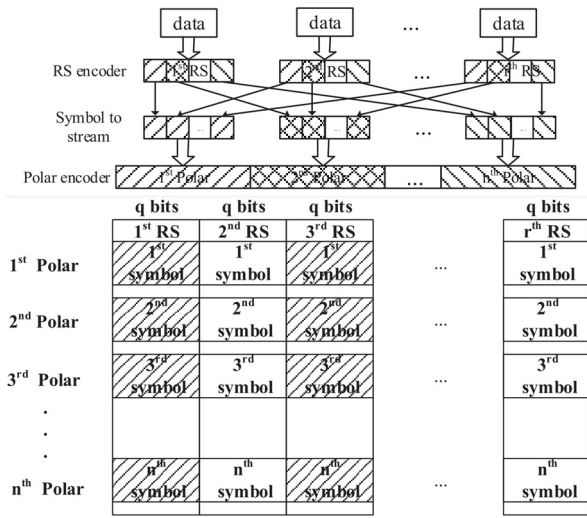


Fig. 2. Proposed polar-RS concatenation scheme [37].

D. 5G Specification

Fig. 3 [38] shows the BER value for a 5G communication system is 10^{-4} when the SNR value is approximately 26 dB [38].

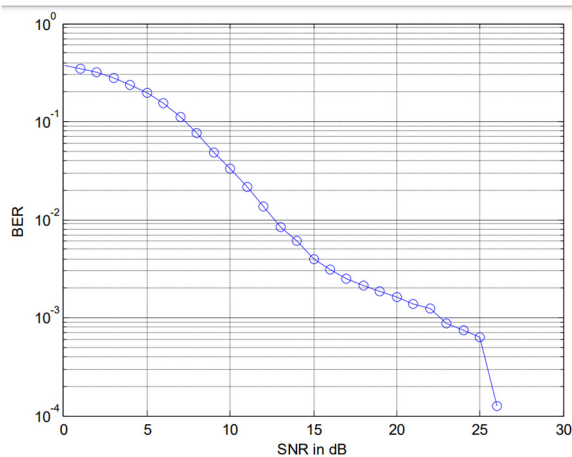


Fig. 3. Bit error rate performance of indoor 5G communication [38].

III. MATERIALS AND METHODS

This research simulates the FEC code performance under AWGN Channel and Burst Error (Gilbert-Elliot) Channel.

A. AWGN Channel Model

The AWGN channel model will use these parameters:

- The ratio of bit energy density and noise energy density (E_b/N_0) that varied from -5 to 25 dB
- The ratio of symbol gain and noise energy density (E_s/N_0) can be formulated by:

$$\frac{E_s}{N_0} = 10 \log_{10}(q) \quad (1)$$

where, q is the number of bits per symbol of channel coding.

- The ratio of symbol gain and noise energy density (E_c/N_0) can be formulated by:

$$\frac{E_c}{N_0} = 10 \log_{10}(R) \quad (2)$$

where, R is the coding rate of the FEC.

B. Gilbert-Elliot Channel Model

Gilbert-Elliot has two states, which are a good state and a bad state. The good state is simulated by an AWGN channel that has a greater value of the ratio of bit energy density and noise energy density (E_b/N_0), whereas the bad state is simulated by an AWGN with a lesser value of the ratio of bit energy density and noise energy density (E_b/N_0).

The change in the channel's state is determined by the set of probabilities shown in Table I. This change of state will simulate a burst error on signal transmission.

The difference value between good and bad states can be formulated by:

$$\frac{E_b}{N_{0b}} = \frac{E_b}{N_{0g}} - 10dB \quad (3)$$

Hence, the parameter of the Gilbert-Elliot Channel Model can be described as

1) Good State

- the ratio of bit energy density and noise energy density (E_b/N_0) that varied from -5 to 25 dB
- the ratio of symbol gain and noise energy density (E_s/N_0) can be formulated by:

$$\frac{E_s}{N_0} = 10 \log_{10}(q) \quad (4)$$

where q is the number of bits per symbol of channel coding.

- The ratio of coding gain and noise energy density (E_s/N_0) can be formulated by:

$$\frac{E_c}{N_0} = 10 \log_{10}(R) \quad (5)$$

2) Bad State

- the ratio of bit energy density and noise energy density (E_b/N_0) that varied from -15 to 15 dB
- The ratio of symbol gain and noise energy density (E_s/N_0) can be formulated by Eq. (4).

- The ratio of coding gain and noise energy density (E_s/N_o) can be formulated by Eq. (5).

TABLE I. PROBABILITIES OF GILBERT-ELLIOT CHANNEL STATE CHANGE

Probabilities	Value
p10	0.1
p01	0.01
p11	0.99
p00	0.9

C. Reed-Solomon Code Architecture

The Reed-Solomon Code Architecture is designed using GV Bound, and Singleton bound as the interval for the code rate used in each architecture.

By using those algorithms, various architectures of Reed Solomon Code can be tabulated to become Table II

TABLE II. REED-SOLOMON CODE ARCHITECTURE

Notation	#Messageword	#Codeword	Error Correction Probability
RS (63,56)	56	63	3
RS (63,55)	55	63	4
RS (63,53)	53	63	5
RS (31,28)	28	31	1
RS (31,26)	26	31	2
RS (31,25)	25	31	3
RS (15,13)	13	15	1
RS (15,11)	11	15	2
RS (15,10)	10	15	3

The Reed-Solomon Code Architecture is designed by using Gallois-Varshamov (GV) Bound, and Singleton bound as the interval for the code rate used in each architecture.

For an RS Code with a codeword length of 63 bits, we can calculate the code bound using Singleton Bound that can be formulated by:

$$d \leq n - k + 1 \quad (6)$$

The other bound that is used is the GV bound, which is formulated by:

$$R \geq 1 - \frac{\log_q \left(\sum_{j=0}^{q-1} \binom{n}{j} (q-1)^j \right) - 1}{n} \quad (7)$$

D. Polar-RS Concatenation

RS Code is used as the outer layer of the FEC concatenation method and Polar Code is used as the inner layer of the FEC concatenation method [14]. The codeword produced by the RS Encoder is interleaved before entering the Polar Encoder [14]. This method will increase the performance of this FEC Concatenation method. Fig. 2 describes the architecture of said FEC concatenation method proposed in this paper.

E. Simulated Model for BER Measurement

In this paper, the BER performance of RS Code and LDPC is measured in four different scenarios which are BER measurement for variation of RS Code Architectures, BER measurement for variation of channel modulations (Quadrature Phase Shift Keying (QPSK), 16 Quadrature

Amplitude Modulation (QAM), 64 QAM), BER measurement for Polar-RS and LDPC, and BER measurement using an image as input data.

The algorithm shown in Fig. 4 can be explained by these steps:

- Random binary data with the size of 10,000 bits are generated.
- Zeros will be added to the end of the binary data to match the architecture of the Reed-Solomon Code.
- The data will be modulated with the chosen modulation method (QPSK/16 QAM/ 64 QAM);
- The modulated signal will be transmitted through the channel (AWGN/Gilbert-Elliott);
- The affected signal will be demodulated with the same modulation method that has been used to modulate the signal.
- The data from demodulation will be decoded with the FEC decoder to recover the original message.
- Recovering the data by removing the trailing zero.
- The recovered data will be compared with the original data to determine the BER value.

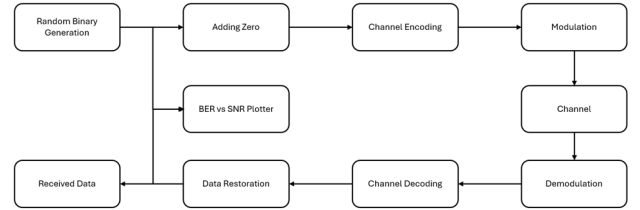


Fig. 4. Simulated system for bit error rate measurement.

F. Simulated Model for BER Measurement

In this paper, the throughput performance of Polar-RS Code and LDPC are measured by simulating the 5G PDSCH system that transmits the signal through AWGN and Gilbert-Elliott Channel. The parameter used by this simulation is listed in Table III.

The algorithm shown in Fig. 5 can be explained by these steps:

- Random binary data with the size of 100 bits representing 1 transport block are generated.
- Generate 10 transport blocks.
- Zeros will be added to the end of the binary data to match the architecture of the Reed-Solomon Code.
- The data will be coded in the Downlink Shared Channel (DL-SCH) block that includes the tested FECs which are LDPC and Polar-RS Code.
- The coded data will be modulated in a PDSCH block that includes QPSK Modulation with one layer of PDSCH so that one layer is composed of one codeword. The Number of Resource Block (NRB) used in this simulation is 52.
- The Sub-Carrier Spacings of the PDSCH block are varied with the values of 15, 30, 60, 120, and 240 kHz.
- The modulated signal will be transmitted through the channel (AWGN/Gilbert-Elliott);

- The affected signal will be demodulated with the PDSCH Decode.
- The data from demodulation will be decoded with the FEC decoder in the DL-SCH Decoder to recover the original message.
- Recovering the data by removing the trailing zero.

The recovered data will be compared with the original data to determine the ratio of the recovered bit number and the total transmitted bit (throughput).

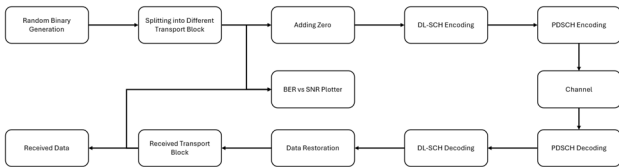


Fig. 5. Simulated system for throughput measurement.

TABLE III. PARAMETERS OF 5G NR POLAR CODE

Parameter	Value
Rate Matched Output Length	30,000 bits (3 times the message bits)
Interleaved Input	True
Cyclic Redundancy Check (CRC) Length	24 bits

IV. RESULT AND DISCUSSION

Simulation is done by using parameters and algorithms explained in Chapter III. The simulation result will be divided into five different sections for different cases used in the simulation. The LDPC code rate used in this simulation is 490/1024.

A. BER Measurement of Various Reed-Solomon Code

The BER values are measured by simulating various Reed-Solomon Code Architecture listed in Table II through the AWGN channel and Gilbert-Elliott Channel

Fig. 6 shows that Reed-Solomon Code has better BER performance than LDPC. The RS Architectures which have the best BER performance are RS (31, 25) and RS (15, 11). They have a BER of 10^{-8} when the Eb/No is equal to 7dB. Comparing that to LDPC which has a BER of 10^{-8} when the Eb/No is equal to 14 dB, it can be shown that LDPC has lesser BER performance than RS Code on AWGN Channel.

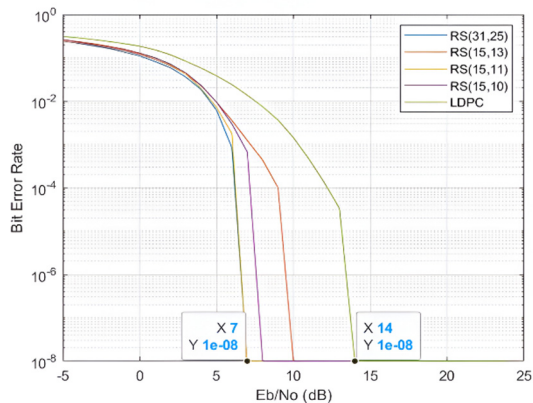


Fig. 6. Bit error rate vs Eb/No result of various reed-solomon architecture on AWGN channel.

Fig. 7 shows that Reed-Solomon Code has better BER performance than LDPC. The RS Architectures which have the best BER performance is RS (63,53) which has a BER of 10^{-8} when the Eb/No is equal to 7dB. Comparing that to LDPC which has a BER of 10^{-8} when the Eb/No is equal to 14 dB, it can be shown that LDPC has lesser BER performance than RS Code on AWGN Channel.

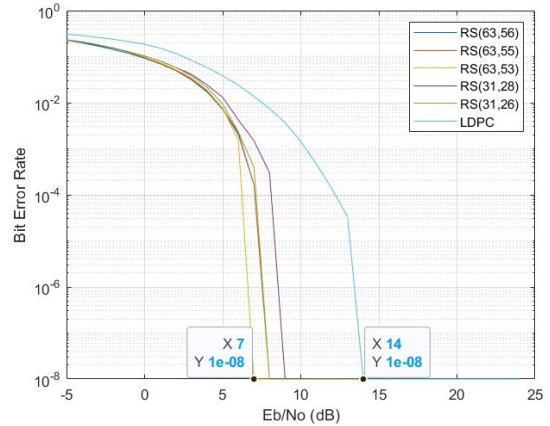


Fig. 7. Bit error rate vs Eb/No result of various RS architecture on AWGN channel.

It can be seen from Figs. 6 and 7, that The Reed-Solomon Codes Architectures have a larger difference between their number of codewords and the number of messagewords have a better BER performance than the others. This happened because the bigger the difference between the number of codewords and number of messagewords the more parity check bit that can be used to correct the transmitted data.

Fig. 8 shows that Reed-Solomon Code has better BER performance than LDPC. The RS Architectures which have the best BER performance are RS (31, 25) and RS (15, 11). They have a BER of 10^{-8} when the Eb/No is equal to 15dB. Comparing that to LDPC which has a BER of 10^{-8} when the Eb/No is equal to 24dB, it can be shown that LDPC has lesser BER performance than RS Code on Gilbert Elliot Channel.

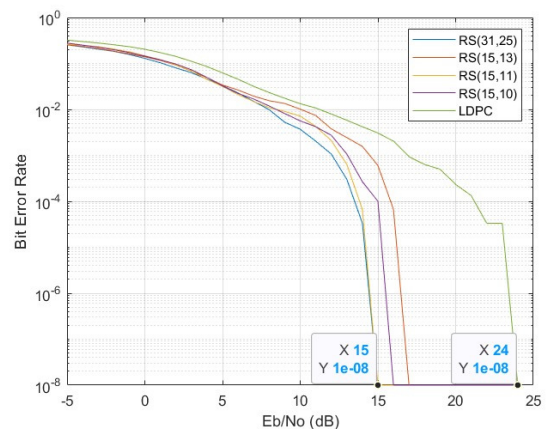


Fig. 8. Bit error rate vs Eb/No result of various RS architecture in gilbert-elliott channel.

Fig. 9 shows that Reed-Solomon Code has better BER performance than LDPC. The RS Architectures that have

the best BER performance is RS (63, 53) which has a BER of 10^{-8} when the E_b/N_0 is equal to 13dB. Comparing that to LDPC which has a BER of 10^{-8} when the E_b/N_0 is equal to 24 dB, it can be shown that LDPC has lesser BER performance than RS Code on AWGN Channel.

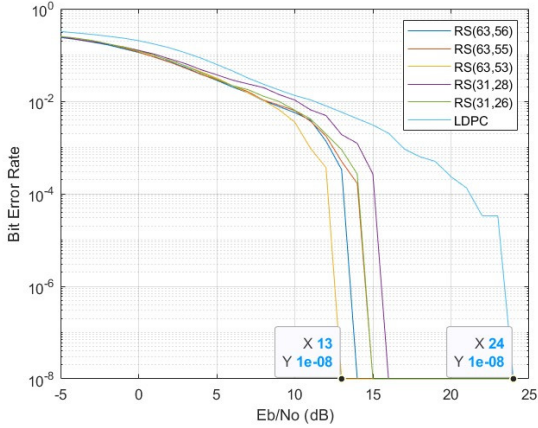


Fig. 9. Bit error rate vs E_b/N_0 result of various RS architecture in Gilbert-Elliot channel.

The Reed Solomon Code architecture difference phenomenon mentioned in section A can also be seen in Figs. 8 and 9. This means the Reed Solomon Code architecture will affect the BER performance in both AWGN Channel and Gilbert-Elliot Channel.

B. BER Measurement of Various Modulation Methods

The BER measurement, in this case, is using RS Code with the architecture of RS (63, 56) and RS (15, 10) as the FEC that will be modulated with (QPSK, QAM16, and QAM64). This modulated signal then will be transmitted on AWGN and Gilbert-Elliot Channel.

Fig. 10 shows that QPSK has better BER performance than other modulation techniques. Viewed from RS (63, 56), QPSK has a BER of 10^{-8} when the E_b/N_0 is equal to 8 dB. Comparing that with QAM16 which has a BER of 10^{-8} when the E_b/N_0 is equal to 12 dB and QAM64 has a BER of 10^{-8} when the E_b/N_0 is equal to 16 dB, it can be shown that QPSK has a superior BER performance than the other modulation on the AWGN channel.

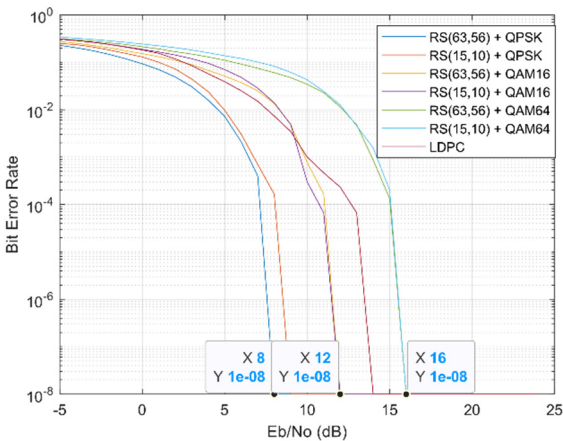


Fig. 10. Bit error rate vs E_b/N_0 result of various modulation techniques in AWGN channel.

Fig. 11 shows that QPSK has better BER performance than other modulation techniques. Viewed from RS (63, 56), QPSK has a BER of 10^{-8} when the E_b/N_0 is equal to 14 dB. Comparing that with QAM16 which has a BER of 10^{-8} when the E_b/N_0 is equal to 18 dB and QAM64 has a BER of 10^{-8} when the E_b/N_0 is equal to 24 dB, it can be shown that QPSK has a superior BER performance than the other modulation on the Gilbert-Elliot channel. As can be seen in Figs. 10 and 11, the modulation technique that has fewer bits per symbol has a better BER performance. This happened because the more bits per symbol that are carried in a signal, the bigger the possibility of the signal being interpreted wrongly on the receiver side. But higher order modulation means more data to be transferred in a certain amount of time. So, to ensure optimum network performance, the right combination of the forward error correction method and the modulation method is needed. Based on Figs. 10 and 11, RS (63,56) + QPSK is the best combination.

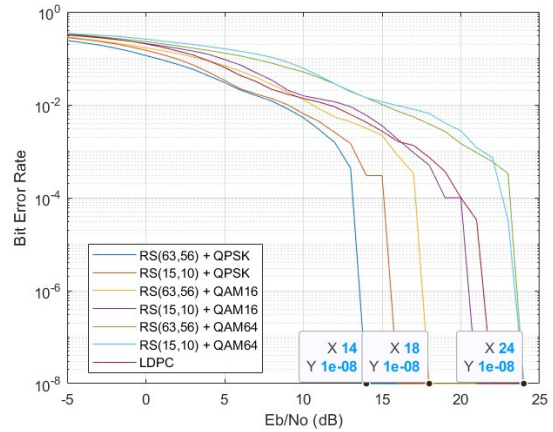


Fig. 11. Bit error rate vs E_b/N_0 result of various modulation techniques in Gilbert-Elliot channel.

C. BER Measurement of RS Code, Polar-RS Code, and LDPC

The BER measurement, in this case, is using a concatenation of RS Code (15, 10) – Polar Code with a code rate of 1/3, RS (63, 56), and LDPC as the FEC that will be modulated with QPSK. This modulated signal then will be transmitted on AWGN and Gilbert-Elliot Channel.

Fig. 12 shows that Polar-RS has better BER performance than RS Code and LDPC. Polar-RS has a BER of 10^{-8} when the E_b/N_0 is equal to 0 dB. Comparing that with other FEC, RS (63, 56) has a BER of 10^{-8} when the E_b/N_0 is equal to 8 dB, and LDPC has a BER of 10^{-8} when the E_b/N_0 is equal to 13 dB, it can be shown that Polar-RS has superior BER performance than the other FEC on the AWGN channel.

Fig. 13 shows that Polar-RS has better BER performance than RS Code and LDPC. Polar-RS has a BER of 10^{-8} when the E_b/N_0 is equal to 4 dB. Comparing that with other FEC, RS (63, 56) has a BER of 10^{-8} when the E_b/N_0 is equal to 15dB, and LDPC has a BER of 10^{-8} when the E_b/N_0 is equal to 21 dB, it can be shown that Polar-RS has superior BER performance than the other FEC on the Gilbert-Elliot channel.

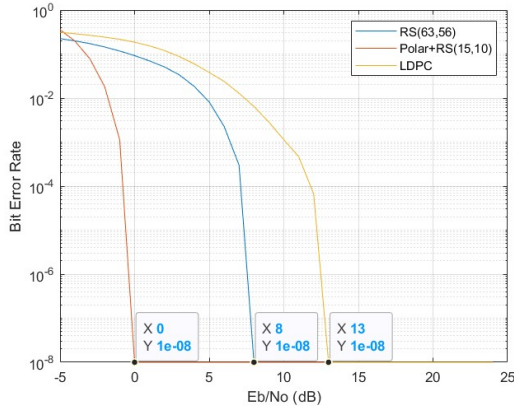


Fig. 12. Bit error rate vs Eb/No result of polar-RS, RS, and low-density parity check in AWGN channel.

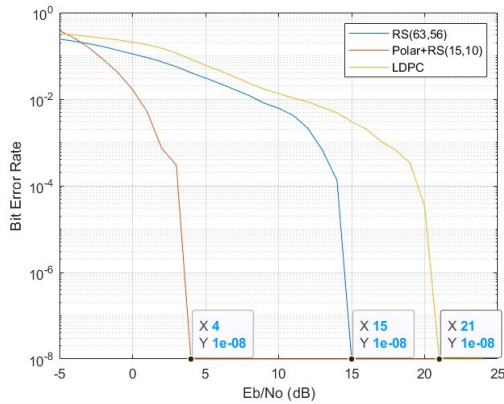


Fig. 13. Bit error rate vs Eb/No result of polar-RS, RS, and low-density parity check in Gilbert-Elliot channel.

As seen in Figs. 12 and 13, The BER performance of the Polar-RS concatenation is superior to both RS and LDPC Code. This phenomenon happened because the correction capability of Polar Code combined with the burst error correction of RS Code resulted in an FEC method that has great error correcting capability in AWGN Channel (Single bit error) and Gilbert-Elliot Channel (Burst Error). However, this FEC method has a disadvantage which is the long processing time. The concatenation means that the system will do both Polar Code and RS code in the decoder and encoder, and that requires a lot more time. Hence further research is needed to optimize this FEC scheme. In the meanwhile, the long processing time is compensated for by the usage of high-performance processors.

As seen in Table IV, the concatenated codes have superior performance than the single codes. The concatenated codes will have two or more coding methods to secure the data hence better BER performance.

Compared to other studies tabulated in Table IV, Polar + RS (15, 10) has a superior performance compared to other error-correcting methods. The Polar-RS code has great error-correcting capability from RS code and low coding complexity from Polar-RS code. The Quadrature Phase Shift Keying (QPSK) modulation also helps the BER performance of the Polar-RS because it can carry more data hence it can be more resilient in the AWGN channel compared to BPSK which is used by the other studies.

TABLE IV. BER COMPARISON FOR VARIOUS ERROR CORRECTING METHODS ON AWGN CHANNEL

Error Correcting Method	BER Value @ Eb/No=3 dB
RS(63, 56){QPSK}	$\approx 2 \cdot 10^{-2}$
Polar+RS(15, 10){QPSK}	$< 10^{-8}$
LDPC{QPSK}	$\approx 7 \cdot 10^{-2}$
BCH(31, 16)+BI+LDPC(32, 16){BPSK}(13)	$\approx 3 \cdot 10^{-4}$
BCH(31, 16)+BI+Polar(32, 16){BPSK}(13)	$\approx 2 \cdot 10^{-5}$
BCH(31, 16)+BI+Turbo(32, 16){BPSK}(13)	$< 10^{-6}$
Turbo 5-it(12)	$\approx 7 \cdot 10^{-6}$

D. Throughput Measurement of RS Code, Polar-RS Code, and LDPC on 5G PDSCH System

The throughput value is measured by calculating the ratio of the number of bits in a successfully received transport block and the total number of transmitted bits. In this measurement, the Sub-Carrier Spacing of the PDSCH block is varied to determine the effect of Sub-Carrier Spacing (SCS) value on throughput performance.

Fig. 14 shows that the throughput of Polar-RS Code is superior to LDPC. The throughput rise over the increasing value of Eb/No on Polar-RS has a steeper rise than the LDPC. This can be interpreted as Polar-RS having better performance in correcting the error than LDPC in the AWGN channel.

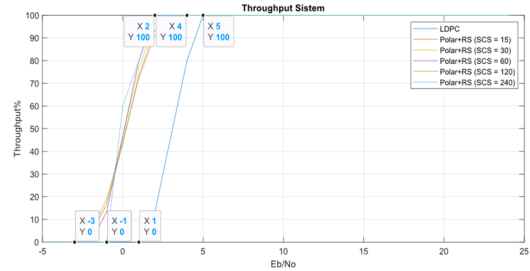


Fig. 14. Throughput result of simulated PDSCH on AWGN channel.

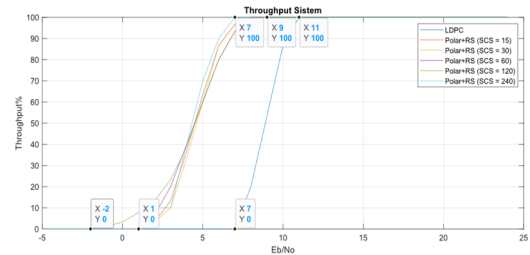


Fig. 15. Throughput result of simulated PDSCH on Gilbert-Elliot channel.

The SCS value of 240 kHz has the best throughput performance with a throughput value of 100 % at Eb/No equals 2dB.

Fig. 15 shows that the throughput of Polar-RS Code is superior to LDPC. The throughput rise over the increasing value of Eb/No on Polar-RS has a steeper rise than the LDPC. This can be interpreted as Polar-RS having better performance in correcting the error than LDPC in the AWGN channel.

The SCS value of 240 kHz has the best throughput performance with a throughput value of 100 at Eb/No equals 6dB.

The throughput percentage is related to the BER value as can be analyzed in Figs. 14 and 15. As E_b/N_0 value increases the throughput percentage also increases. This happened because as the E_b/N_0 value increases, more correct data can be received hence throughput value will increase too.

SCS values can also affect the throughput percentage. Bigger SCS will make the throughput performance better. But, based on Figs. 14 and 15 the biggest SCS value of 240 kHz doesn't result in the best throughput percentage performance. This happened because a bigger SCS value means a bigger gap between each sub-carrier, making it carry less data. Hence, the SCS value of 120 kHz is the most optimum SCS value for the simulated system.

V. CONCLUSION

The BER performance shows that RS Code has better error-correcting capability than LDPC code. This advantage is further enhanced by concatenating RS Code with Polar Code. This concatenation results in an FEC method with the best error-correcting capability than the other FEC methods measured in this paper.

The BER performance of the Burst Error Scenario simulated through the Gilbert-Elliott Channel shown in Figs. 8 and 9 shows that RS code encoding has superior performance than LDPC

The BER performance of both the RS code and Polar-RS code has fulfilled the 5G specification shown in Fig. 3, hence RS code and Polar-RS code were determined to be a good candidate for the future release of 5G communication.

The throughput percentage shows how much data that successfully transmitted through the channel. As we can see in Figs. 14 and 15 the Polar + RS Code has a higher throughput percentage at lower E_b/N_0 values. It shows that the Polar + RS Code can make the transmission in the AWGN and Gilbert-Elliott (Burst Error) Channels better. In the practical application of 5G Transmission, using the Polar + RS Code system will have better performance.

5G PDSCH system which uses Polar-RS as its DL-SCH encoder shows better throughput performance than the LDPC counterpart. The best SCS value of said PDSCH is 240 kHz.

The Simulated BER and Throughput performance of Polar-RS Code shows the potential of these schemes to be used in 5G Transmission. A lower BER value means more robust transmission with a low chance of retransmission of the data. This allows high rate and low latency transmission.

This research shows that the Polar-RS code has better BER and Throughput performance for both the AWGN channel and Burst Error Channel compared to LDPC which is used in the current 5G transmission. This model can be proposed for the next 5G release or the next generation of mobile telecommunication.

CONFLICT OF INTEREST

The authors declare no conflict of interest.

AUTHOR CONTRIBUTIONS

Prof. Muh Asvial and Primayoga conducted the research; Prof Muh. Asvial analyzed the data; Primayoga built the simulation and wrote the paper; all authors had approved the final version.

REFERENCES

- [1] S. Tabbane, "4G to 5G networks and standard releases," *3GPP*, October 2019.
- [2] 3GPP. (2023). Introducing 3GPP. [Online]. Available: <https://www.3gpp.org/about-us/introducing-3gpp>
- [3] X Lin, "An overview of 5g advanced evolution in 3gpp release 18," *IEEE Communications Standards Magazine*, vol. 6, no. 3, pp. 77–83, 2022. <https://doi.org/10.1109/MCOMSTD.0001.2200001>
- [4] M. I. Manda and S. B. Dhaou, "Responding to the challenges and opportunities in the 4th Industrial revolution in developing countries," in *Proc. the 12th International Conference on Theory and Practice of Electronic Governance*, 2019, pp. 244–253. <https://doi.org/10.1145/3326365.3326398>
- [5] M. Barberis, "Understanding and modeling the 5G NR physical layer," *MATLAB Expo 2019*, 2019.
- [6] A. Hanan, "Chapter 8 OSI physical layer," Al-Mustansiriyah University, Faculty of Engineering, Computer Networks Computer Engineering Department, 2016–2017.
- [7] F. H. El-Fouly, R. A. Ramadan, F. E. Abd El-Samie, M. Kachout, A. J. Alzahrani, and J. S. Alshudukhi, "Burst channel error reduction based on interleaving for efficient high-speed wireless communication," *Journal Applied Sciences*, 2022. <https://doi.org/10.3390/app12073500>
- [8] N. Naimipour, H. Safavi, and H. Shaw, "Polar coding for forward error correction in space communications with LDPC comparisons," in *Proc. International Astronautical Congress 2019*, Location: Washington, D.C., 2019.
- [9] International Civil Aviation Organization. (2014). Aeronautical Communications Panel (ACP) 15th April Webmeeting of the Working Group S (Surface). [Online]. Available: [https://www.icao.int/safety/acp/ACPWG/ACP-WG-S-Web%20Meeting%205/ACP-WG-S_WP04-ErrorMeasurement_r11%20%20\(2\).docx](https://www.icao.int/safety/acp/ACPWG/ACP-WG-S-Web%20Meeting%205/ACP-WG-S_WP04-ErrorMeasurement_r11%20%20(2).docx)
- [10] 3GPP. (2018). 5G NR Multiplexing and channel coding (3GPP TS 38.212 version 15.2.0 Release 15). [Online]. Available: https://www.etsi.org/deliver/etsi_ts/138200_138299/138212/15.02_00_60/ts_138212v150200p.pdf
- [11] ETSI, 5G NR Physical layer General Description. (2018). [Online]. Available: https://www.etsi.org/deliver/etsi_ts/138200_138299/138201/15.00_00_60/ts_138201v150000p.pdf
- [12] 3GPP, 5G NR User Equipment (UE) Conformance Specification; Radio Transmission and Reception; Part 4: Performance (3GPP TS 38.521-4 version 15.0.0 Release 15) 5G NR User Equipment (UE) conformance specification; Radio transmission and reception; Part 4: Performance (3GPP TS 38.521-4 version 15.0.0 Release 15), (2019). [Online]. Available: https://www.etsi.org/deliver/etsi_ts/138500_138599/13852104/15.00_00_60/ts_13852104v150000p.pdf
- [13] 3GPP, 5G study on scenarios and requirements for next generation access technologies (3GPP TR 38.913 version 14.2.0 release 14). (2017). [Online]. Available: https://www.etsi.org/deliver/etsi_tr/138900_138999/138913/14.02_00_60/tr_138913v140200p.pdf
- [14] A. Ghosh. *5G New Radio (NR): Physical Layer Overview and Performance IEEE Communication Theory Workshop—2018*. [Online]. Available: <https://wp-files.comsoc.org/ctw-2018/files/2018/05/5G-NR-CTW-final.pdf>
- [15] S. Belhadj and M. L. Abdelmounaim, "On error correction performance of LDPC and polar codes for the 5G machine type communications," in *Proc. 2021 IEEE International IOT, Electronics and Mechatronics Conference (IEMTRONICS)*, 2021, pp. 1–4. doi: 10.1109/IEMTRONICS52119.2021.9422665
- [16] A. M. Veresova and A. A. Ovchinnikov, "Comparison of the probability of reed—SOLOMON and LDPC codes decoding error in the gilbert—ELLIOTT channel," in *Proc. 2022 Wave Electronics*

- and Its Application in Information and Telecommunication Systems (WECONF), 2022, pp. 1–4. <https://doi.org/10.1109/WECONF55058.2022.9803501>
- [17] E. N. Gilbert, “Capacity of a burst-noise channel,” *Bell System Technical Journal*, vol. 39, no. 5, pp. 1253–1265, 1960. <https://doi.org/10.1002/j.1538-7305.1960.tb03959.x>
- [18] An introduction to Reed-Solomon codes: Principles, architecture and implementation. (1998). [Online]. Available: https://www.cs.cmu.edu/~guyb/realworld/reedsolomon/reed_solo_mon_codes.html
- [19] I. S. Reed and G. Solomon, “Polynomial codes over certain finite fields,” *J. Soc. Indust. Appl. Math.*, vol. 8, no. 2, 1994.
- [20] S. B. Wicker and V. K. Bhargava, “An introduction to reed-solomon code,” *Reed-Solomon Codes and Their Applications*, Wiley-IEEE Press, 1994.
- [21] C. Zhao, F. Yang, C. Chen, and R. Umar, “Reed-Solomon coded cooperative space-time block coded spatial modulation,” in *Proc. 2021 International Conference on Wireless Communications and Smart Grid (ICWCSG)*, Hangzhou, China, 2021, pp. 99–103. doi: 10.1109/ICWCSG53609.2021.00027
- [22] N. Tang and Y. Lin, “Fast encoding and decoding algorithms for Arbitrary (n,k) Reed-Solomon codes over $F_{(2^m)}$,” *IEEE Communications Letters*, vol. 24, no. 4, pp. 716–719, 2020. <https://doi.org/10.1109/LCOMM.2020.2965453>
- [23] V. Guruswami. (2010). Notes 2: Gilbert-Varshamov bound. CMU. [Online]. Available: <https://www.cs.cmu.edu/~venkatg/teaching/codingtheory/notes/notes2.pdf>
- [24] V. Guruswami. (2010). Notes 4: Elementary bounds on codes. CMU. [Online]. Available: <https://www.cs.cmu.edu/~venkatg/teaching/codingtheory/notes/notes4.pdf>
- [25] S. Ball. (2019). Maximum distance separable codes: Recent advances and applications. Universitat Politècnica Catalunya. [Online]. Available: <https://bgsmath.cat/wp-content/uploads/2019/04/SimeonBall.pdf>
- [26] A. Mazumdar. (2017). Lecture 5, compsci 690t coding theory and applications. [Online]. Available: <https://people.cs.umass.edu/~arya/courses/690T/lecture5.pdf>
- [27] J. G. Proakis and M. Salehi, *Digital Communications*, 5th ed., McGraw-Hill, 2008.
- [28] T. S. Rappaport, *Wireless Communications: Principles and Practice*, 2nd ed., Prentice Hall PTR, 2002.
- [29] A. W. Eckford, F. R. Kschischang, and S. Pasupathy, “Analysis of low-density parity-check codes for the gilbert–Elliott channel,” *IEEE Transactions on Information Theory*, vol. 51, no. 11, pp. 3872–3889, 2005. <https://doi.org/10.1109/TIT.2005.856934>
- [30] J. Zhao, W. Zhang, Y. Liu, J. Gao, and R. Zhang, “A rate-matching concatenation scheme of polar codes with outer reed-Solomon codes,” *IEEE Wireless Communications Letters*, vol. 10, no. 3, pp. 459–463, 2021. <https://doi.org/10.1109/LWC.2020.3033850>
- [31] S. K. Parvathy, K. Rasadurat, and N. Kumaratharan, “LDPC coding for performance enhancement of MC-CDMA system,” *International Journal of Advanced Trends in Computer Science and Engineering*, vol. 2, no. 1, 2013.
- [32] S. Mahajan and G. Singh, “Reed-Solomon code performance for M-ary Modulation over AWGN Channel,” *International Journal of Engineering Science and Technology*, vol. 3, no. 5, 2011.
- [33] C. Zhao, F. Yang, C. Chen, and R. Umar, “Reed-Solomon coded cooperative space-time block coded spatial modulation,” in *Proc. 2021 International Conference on Wireless Communications and Smart Grid (ICWCSG)*, Hangzhou, China, 2021, pp. 99–103. doi: 10.1109/ICWCSG53609.2021.00027
- [34] D. T. Nguyen and Y. Park, “Performance analysis of polar coding and ldpc coding in optical camera communications,” in *Proc. KICS Conference*, 2019.
- [35] Q. Wang, P. Fu, and S. Zhang, “A comparison of concatenated polar codes with different interleaving and decoding schemes,” in *Proc. 2020 5th International Conference on Computer and Communication Systems (ICCCS)*, 2020, pp. 570–574. <https://doi.org/10.1109/ICCCS49078.2020.9118473>
- [36] J. H. Kang, W. Stark, and A. Hero. (1999). Turbo codes for fading and burst channel. [Online]. Available: https://www.researchgate.net/publication/2417101_Turbo_Codes_for_Fading_and_Burst_Channels
- [37] Y. Wang, W. Zhang, Y. Liu, L. Wang, and Y. Liang, “An improved concatenation scheme of polar codes with reed–Solomon codes,” *IEEE Communications Letters*, vol. 21, no. 3, pp. 468–471, 2017. <https://doi.org/10.1109/LCOMM.2016.2639482>
- [38] B. Arora, P. Chawla, and R. Budhiraja, “BER analysis and specifications of future generation coalescing 5G and cognitive radio,” *International Journal of Computer Applications*, vol. 89, no 13, pp. 21–27, 2014. <https://doi.org/10.5120/15691-4569>

Copyright © 2024 by the authors. This is an open access article distributed under the Creative Commons Attribution License ([CC BY-NC-ND 4.0](https://creativecommons.org/licenses/by-nc-nd/4.0/)), which permits use, distribution and reproduction in any medium, provided that the article is properly cited, the use is non-commercial and no modifications or adaptations are made.